

Water Temperature Model: A Case Study in Alagoinhas-BA

Carmen Gonçalves de Macêdo e Silva^{1*}, Marcos Batista Figueredo¹

¹UNEB, PPGMSB; Alagoinhas, Bahia, Brazil

In recent years, climate change has generated disturbances at both local and global scales, directly impacting the water temperature of rivers. Temperature fluctuations have become a common occurrence in river water, where after experiencing heating, the return to its natural temperature is gradual. Consequently, temperature changes affect various internal processes within rivers, including nutrient consumption, food availability, and dissolved oxygen concentration. These alterations subsequently impact the growth and distribution of aquatic organisms. This article focuses on the physical variables derived from a model characterized by limited computational complexity. The final structure of the model consists of a single ordinary differential equation, which is linearly dependent on air and water temperature, as well as flow rate. Additionally, to handle data sequences such as time series more efficiently than traditional Recurrent Neural Networks (RNNs), we employ a Long Short-Term Memory (LSTM) neural network.

Keywords: Temperature. River. Water.

Introduction

In recent years, climate change has caused disturbances at both local and global scales [1], directly impacting the water temperature of rivers. Temperature fluctuations are common in river water, wherein heated water returns gradually to its natural temperature [2].

Anthropogenic activities such as thermal pollution, deforestation, and climate change are typically responsible for changes in river temperature [3]. Natural factors also contribute to temperature variations, including changes in geothermal heat energy, seasonal fluctuations in ambient temperature and insolation, and alterations in river flow. The surface water temperature is further influenced by latitude, altitude, season, air circulation, cloud cover, flow rate, and water body depth [4]. These factors affecting river temperature can be categorized into atmospheric conditions, topography, flow dynamics, and riverbed characteristics [5]. Generally, the average daily temperature

increases downstream and tends to rise with distance and flow [6-8].

Consequently, temperature changes affect other internal processes within rivers, such as nutrient consumption, food availability, and dissolved oxygen concentration [9, 10], impacting aquatic organisms' growth and distribution [11-14]. Moreover, water chemistry is influenced by temperature, as it affects density, leading to stratified water layers that do not mix, particularly evident in surface waters affected by latitude and altitude [15].

It is evident that a comprehensive understanding of the thermal regime of rivers is crucial for efficient environmental management and conducting environmental impact assessments [16]. Therefore, computer models predicting river water temperature are utilized. Numerous models have been developed for estimating river water temperature, including deterministic and statistical models. Deterministic models rely on energy balance principles and necessitate a considerable amount of input data. In contrast, statistical models correlate water temperature with another variable, enabling a mathematical description of their relationship. Given their similar temporal evolution, one such highly correlated variable is air temperature, making it regular to apply statistical regression models between these two variables [17].

Received on 18 November 2023; revised 8 December 2023.
Address for correspondence: Carmen Gonçalves de Macêdo e Silva. BR 110, Km 03, Alagoinhas. Zipcode: 48.000.000. Alagoinhas, Bahia, Brazil. E-mail: carmen.fest@outlook.com.

J Bioeng. Tech. Health 2023;6(Suppl 2):66-70
© 2023 by SENAI CIMATEC. All rights reserved.

This article focuses on the physical variables derived from a model characterized by limited computational complexity. The final structure entails a single ordinary differential equation linearly dependent on air and water temperature and flow [18]. Additionally, we employ a Long Short-Term Memory (LSTM) neural network designed to handle data sequences, such as time series, more efficiently than traditional Recurrent Neural Networks (RNNs).

Materials and Methods

The simple linear regression employed to predict water temperature utilizes only air temperature as input data, with data collected every month. The resulting model is grounded on a focused heat balance concept. It considers an unknown volume (V) encompassing the river stretch, its tributaries (implicitly incorporating surface and underground water flows), and heat exchange with the atmosphere. Within this volume, the variation in water temperature is described by Equation 1:

$$\rho C_p V T_w t = AH + \rho C_p (\sum Q_i T_w - QT_w) \quad (1)$$

Where t represents time (expressed in months, weeks, days, or hours), ρ is the density of water, ρC_p is its specific heat capacity at constant pressure, A is the surface area under analysis, H is the heat flux at the river-atmosphere interface, Q is the temperature flux in the surface, Q_i and T_w represent the temperatures of water flow (from tributaries and possibly groundwater), and V denotes the total volume reacting to heat fluxes. This total volume V encompasses not only the surface water body but also the region where surface water contacts deep water, rendering explicit inclusion of heat fluxes at the riverbed interface unnecessary. Moreover, the liquid heat flux H primarily depends on short and long-wave radiation and sensible and latent heat fluxes.

The model assumes that the air temperature can be used in all these processes. The general effect is included in the model linearly using a Taylor series expansion (Equation 2)

$$H = H | \frac{T_a T_w}{T_a T_w} + H T_a \frac{T_a T_w}{T_a T_w} (T_a - \frac{T_a}{T_a} + \frac{T_w - T_w}{T_w}) \quad (2)$$

Where T_a and T_w are the long-term average values (from now on indicated by a bar) of air and water temperatures, respectively. Equation 3 presents this relation

$$H = \rho C_p (h_o + h_a T_a - h_w T_w) \quad (3)$$

Where h_o , h_a , and h_w are parameters that can be directly obtained from the derivative of Equation 3. The second term on the right side of the equation represents the difference between the heat flow coming out of the control volume, $\rho C_p Q T_w$ and the sum of all heat flow inputs. The work of Toffolon & Piccolroaz (2015) [18] rewrote the equation presented in Cassie (2005) [19] and obtained Equation 4 below:

$$T_w t = \frac{A}{V} (h_o + h_a T_a - h_w T_w) + \frac{Q}{V} (\hat{T} - T_w) \quad (4)$$

As the reference temperature will likely change in different seasons to T_w , it was expressed as a first approximation in the form of annual sinusoidal variation (Equation 5).

$$\hat{T}_w = \hat{T}_{w0} + \hat{T}_{w1} 2\pi (\frac{t}{t_y} - \varphi) \quad (5)$$

Where the reference value \hat{T}_{w0} has variation in amplitude, \hat{T}_{w1} and φ [0,1] q , which contains two characteristic quantities. The inverse of the first ratio, $\frac{V}{A}$, is related to the depth of flow (and therefore depends on the flow rate) but does not coincide with it. A portion of the saturated sediments should be included, especially for shallow flows with high transparency, where incident shortwave radiation can directly heat the river bed. The second reason in the equation, $\frac{Q}{V}$, represents the inverse of the time and reach of the river and also varies with the flow.

This article will use an LSTM (Long Short-Term Memory), a recurrent neural network (RNN) designed to handle data sequences, such as time series, more effectively than traditional RNNs.

Figure 1 illustrates the structure of the LSTM cell, comprising three distinct gates: the forget gate,

the input gate, and the output gate. The memory cell, serving as a repository for state information, stands out as the characteristic element of LSTM networks. Upon activation of the input gate, new information is assimilated into the cell, whereas the forget gate triggers the removal of prior data. Within the feedback loop, the sigmoid function determines the information to be retained or forgotten in the memory cell, while the hyperbolic tangent function regulates cell input and output. Through the synergistic integration of these functions, LSTM can selectively retain or discard information, effectively managing time series data and generating predictions.

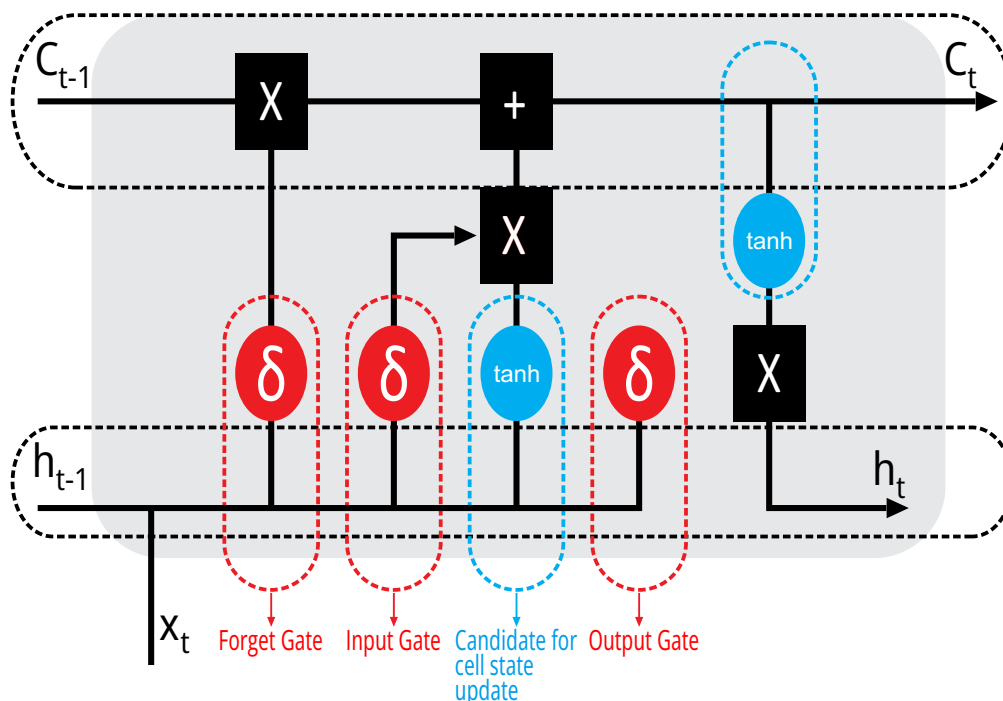
Characterization of the Study Area

The Catu River, situated in Bahia, Brazil, originates from Alagoinhas/Bahia, specifically from the village of Catuzinho. It traverses the Marechal Floriano neighborhood, crosses Catu Street, and flows through commercial areas before skirting the banks of BR 110 near UNEB - Campus II. Continuing its course, it reaches the city of Catu and eventually

merges with the Pojuca River in Pojuca/Bahia. Serving as one of the primary sources of freshwater in the northeastern region of Bahia, the Catu River stretches approximately 120 kilometers, originating from the Serra do Orobó. Its trajectory encompasses urban and rural areas before discharging into the Atlantic Ocean. The river's watershed spans several municipalities, including Alagoinhas, Catu, and Pojuca, underscoring its significance as a vital natural resource for the local populace. Additionally, the Catu River plays a pivotal role in maintaining the ecological equilibrium of the region. Its banks and adjacent areas support diverse biodiversity, comprising various bird species, fish, and aquatic vegetation. Furthermore, its flow contributes to the preservation of groundwater, ensuring the provision of water to the population and safeguarding agricultural lands.

According to Silva and colleagues (2018) [20], similar to many rivers worldwide, the Catu River grapples with severe pollution issues primarily stemming from industrial and urban activities along its course. Improper disposal of solid and liquid waste, coupled with the absence of efficient

Figure 1. Structure of the internal LSTM cell.



sewage treatment systems, significantly contributes to water quality degradation. These activities result in the release of toxic substances, including heavy metals and chemicals, which pose threats to both water quality and aquatic life. Santos (2007) [21] emphasizes the substantial dependence of the local economy on the Catu River.

Fishing stands out as a traditional activity in riverside communities, serving as a vital source of sustenance and income for numerous families. Moreover, irrigated agriculture along the riverbanks supports cultivating crops such as fruits, legumes, and sugarcane. River water is also utilized for livestock husbandry and sustains operations in small-scale industries. However, these activities harm aquatic flora and fauna, leading to species extinction and ecological imbalance. Furthermore, contamination poses health risks to communities reliant on river water for daily needs [22].

The Catu River holds significant cultural importance, serving as the backdrop for festivities, religious ceremonies, and recreational pursuits, enriching riverside communities' cultural heritage. Additionally, the river is a vital transportation artery for people and goods in certain regions, facilitating access to essential services like healthcare and education. Despite its pivotal role, the Catu River faces numerous threats. Water pollution from industrial and domestic waste undermines the river's quality and the well-being of communities dependent on it [22]. Deforestation of riparian forest areas and harmful agricultural practices exacerbate riverbank erosion and siltation. Furthermore, climate change disrupts the rainfall regime, impacting freshwater flow.

Results and Discussion

Figure 2 displays a collection of training data represented in blue, alongside a set of validation data depicted in orange. Upon comparison, it becomes evident that a significant similarity exists between the expected and obtained results, highlighting the effectiveness of the LSTM neural network.

Figure 2. Comparison between expected and obtained results.

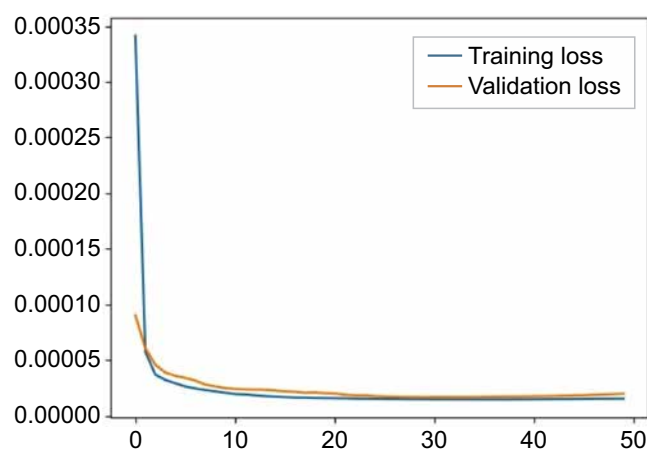


Table 1 presents the performance metrics of the model, including Mean Absolute Error (MAE), Mean Square Error (MSE), Root Mean Square Error (RMSE), and the coefficient of determination (R^2). The MAE value of 0.27 indicates that, on average, the model's forecasts deviate by 0.27 units from the actual values. The MSE of 0.11, close to zero, suggests that the model performed well, with forecasts relatively close to the actual values. The RMSE of 0.33 implies that the model is sensitive to outliers but still provides a reasonable degree of accuracy. However, the coefficient of determination R^2 of -4.84 raises concerns as it indicates a poor fit of the model's predictions to the actual values.

Table 1. Results obtained from the temperature.

Metrics	Value
MAE	0.27
MSE	0.11
RMSE	0.33
R^2	-4.84

Conclusion

In conclusion, the results demonstrate that the LSTM neural network, designed to handle data sequences, has shown significant effectiveness in accurately predicting the water temperature of the

Catu River. Despite some limitations, particularly indicated by the negative R^2 value, neural networks represent a promising approach, considering both accuracy and computational efficiency.

References

1. Sinokrot BA, Stefan HG, McCormick JH et al. Modelling of climate change effects on stream temperatures and fish habitats below dams and near groundwater inputs. *Climatic Change* 1995;30:181–200.
2. Webb BW, Wallig D. Temporal variability in the impact of river regulation on thermal regime and some biological implications. *Freshwater Biology* 1993;29:167-182.
3. Van Vliet MT, Franssen WH, Yearsley JR et al. Global river discharge and water temperature under climate change. *Global Environmental Change* 2013;23(2): 450-464.
4. Georges B. Characterization of the river thermal regime in relation to its environment: a regional approach using in situ sensors in a temperate region (wallonia, belgium). 2022.
5. Gresselin F, Dardaillon B, Bordier C et al. Use of statistical methods to characterize the influence of groundwater on the thermal regime of rivers in normandy, france: comparison between the highly permeable, chalk catchment of the touques river and the low permeability, crystalline rock catchment of the orne river. *Geological Society, London, Special Publications* 2022;517(1):517–2020.
6. Jackson FL, Fryer RJ, Hannah DM, Millar CP, Malcom IA. A spatio-temporal statistical model of maximum daily river temperatures to inform the management of scotland's atlantic salmon rivers under climate change. *Science of The Total Environment*, 612, 1543 - 1558. Retrieved from <https://www.sciencedirect.com/science/article/pii/S0048969717323525> doi: <https://doi.org/10.1016/j.scitotenv.2017.09.010>. 2018.
7. Sang YF. Spatial and temporal variability of daily temperature in the yangtze river delta, China. *Atmospheric Research* 2012;112:12-24. Retrieved from <https://www.sciencedirect.com/science/article/pii/S0169809512001123> doi: <https://doi.org/10.1016/j.atmosres.2012.04.006>. 2012.
8. Torregroza-Espinosa AC, Restrepo JC, Escobar J, Pierini J, Newton A. Spatial and temporal variability of temperature, salinity and chlorophyll4 a in the magdalena river mouth, caribbean sea. *Journal of South American Earth Sciences*, 105, 102978. Retrieved from <https://www.sciencedirect.com/science/article/pii>.
9. Sand-Jensen K, Pedersen NL. Differences in temperature, organic carbon and oxygen consumption among lowland streams. *Freshwater Biology* 2005;50:1927–1937.
10. Markarian RK. A study of the relationship between aquatic insect growth and water temperature in a small stream. *Hydrobiologia* 1980;75:81-95.
11. Jensen AJ. Growth of young migratory brown trout *Salmo trutta* correlated with water temperature in Nowegian river. *Journal of Animal Ecology* 1990;69:1010-1020.
12. Elliot JM, Hurley MA. A functional model for maximum growth of Atlantic salmon parr, *salmo solar*, for two populations in northwest England. *Functional Ecology* 1997;11:592-603.
13. Ebersole JL, Liss WJ, Frissell CA. Relationship between stream temperature, thermal refuge, and rainbow trout, *Oncorhynchus mykiss* abundance in dryland streams in the northwestern United States. *Freshwater Fish Ecology* 2001;10:1–10.
14. Letcher BH, Hocking DJ, O'Neil K, Whiteley AR, Nislow KH, O'Donnel MJ. A hierarchical model of daily stream temperature using airwater temperature synchronization, autocorrelation, and time lags. *PeerJ* 2016;4:1727.
15. Cassie D. The thermal regime of rivers: a review. *Freshwater Biology* 2006;51(8):1389–1406.
16. Larnier K, Roux H, Dartus D, Croze O. Water temperature modeling in the Garonne River (France). *Knowledge and Management of Aquatic Ecosystems* 2010;398(4):1–10.
17. Toffolon M, Piccolroaz S. A hybrid model for river water temperature as a function of air temperature and discharge. *Environmental Research Letters* 2015;10(11):114011.
18. Caissie D.; Satish MG, El-Jabi N. Predicting river water temperatures using the equilibrium temperature concept with application on miramichi river catchments (new brunswick, canada). *Hydrological Processes: An International Journal* 2005;19(11):2137–2159.
19. de Freitas GCS, Peixoto FC, Vianna JR, AS. Simulation of a thermal battery using Phoenixs. *Journal of Power Sources* 2008;179:424-429.
20. Silva JR et al. Rastreamento de fontes de nutrientes em um sistema de retenção várzea-subsuperficial (RSR) e sua contribuição para a manutenção da qualidade da água do rio Catu, Bahia, Brasil. *Monitoramento e Avaliação Ambiental* 2018;190(11):1-21.
21. Santos AB, Lima RS. Diagnóstico ambiental da bacia do Rio Catu - BA, Brasil. *Revista Ambiente & Água* 2007;2(2):27-42.
22. Fundação SOS Mata Atlântica. Atlas dos rios do Brasil: Rio Catu. IBGE. Instituto Brasileiro de Geografia e Estatística (IBGE). (2018). Caderno Geográfico – Bahia 2020.